Comparison of the PU.1 transcriptional regulome and interactome in human and mouse inflammatory dendritic cells

Maaike R. Scheenstra,[*,†,1] Patricia Martínez-Botía,[‡,1] Andrea Acebes-Huerta,[‡] Rutger W.W. Brouwer,[§,¶] Noemí Caballero-Sánchez,[‡] Nynke Gillemans,[¶] Pieter de Bleser,[‖] Benjamin Nota,[*] Iris M. De Cuyper,[*] Vishal Salunkhe,[*] Andrea M. Woltman,[#,2] Lianne van de Laar,[#] Erikjan Rijkers,[**] Jeroen A.A. Demmers,[**] Wilfred F.J. van IJcken,[§,¶] Sjaak Philipsen,[¶] Timo K. van den Berg,[*] Taco W. Kuijpers,[*,††,‡‡] Laura Gutiérrez[*,‡,§§]

[*]*Department of Blood Cell Research, Sanquin Research and Landsteiner Laboratory, Academic Medical Center (AMC), University of Amsterdam, Amsterdam, The Netherlands.*

[†]*Division of Infectious Diseases and Immunology, Department of Biomolecular Health Sciences, Utrecht University, The Netherlands.*

[‡]*Instituto de Investigación Sanitaria del Principado de Asturias (ISPA), Oviedo, Spain.*

[§]*Center for Biomics, Erasmus MC, Rotterdam, The Netherlands.*

[¶]*Department of Cell Biology, Erasmus MC, Rotterdam, The Netherlands.*

[‖]*Department of Biomedical Molecular Biology, Ghent University; Data Mining and Modeling for Biomedicine, VIB Center for Inflammation Research, Ghent, Belgium.*

[#]*Department of Gastroenterology and Hepatology, Erasmus MC University Medical Center, Rotterdam, The Netherlands.*

[**]*Proteomics Center, Erasmus University Medical Center, Rotterdam, The Netherlands.*

[††]*Department of Pediatric Hematology, Immunology and Infectious Disease, Emma Children's Hospital, Amsterdam, The Netherlands.*

[‡‡]*Academic Medical Center, University of Amsterdam, Amsterdam, The Netherlands.*

[§§]*Dept. of Medicine, University of Oviedo, Spain.*

[1]*Equally contributing authors.*

[2]*Current Address: Institute of Medical Education Research Rotterdam, Erasmus MC University Medical Center, Rotterdam, The Netherlands*

Corresponding author: *L. Gutiérrez.*

Email: gutierrezglaura@uniovi.es. Phone: +34 985 10 13 90.

Summary sentence: The comparison of the human and mouse PU.1 regulome and interactome in inflammatory DCs reveals species-specific responses and conserved regulatory features of PU.1.

Short running title: PU.1 regulome and interactome in inflammatory DC

Key words: dendritic cells, transcription factor, transcriptome, interactome, interspecies, PU.1

Abstract (max 250): 249 words

Manuscript (22,000-45,000 characters excluding Methods and refs, including legends): 42,226 characters with no spaces

Figures: 6

Supplementary Files: 1 unit of Supplementary Figures (2) and Tables (3), 4 units of omics datasets on Excel files with datasheets, and Graphical Abstract (max 6 units including Graphical Abstract)

References (max 80): 50

Abbreviations PAGE

BAM – Binary Alignment/Map

BETA - Binding and expression target analysis

CD – Cluster of differentiation

CDS – Coding sequence

ChIP – Chromatin Immunoprecipitation

ChIP-Seq – ChIP Sequencing

DC – dendritic cell

- pDC – plasmacytoid DC
- cDC – conventional DC
- moDC – monocyte derived DC
- BMDC – bone marrow derived DC

DNA – Deoxyribonucleic Acid

ECL – Enhanced chemiluminescence

ETS – E26 transformation specific (transcription factor)

FCS – fetal calf serum

GM-CSF – granulocyte-macrophage colony stimulating factor

GO Term – Gene ontology term

HOMER - Hypergeometric Optimization of Motif EnRichment

HUMOT - Human and Mouse Orthologous Gene Nomenclature

IL-4 – Interleukin 4

KEGG – Kyoto Encyclopedia of Genes and Genomes

LFQ – Label free quantification

LPS - lipopolysaccharide

MACS – Model-based analysis for ChIP-Seq

MEME – Multiple Em for Motif Elicitation MF - macrophage

MF - Macrophage

MHC-II – Major histocompatibility complex II

PANTHER - Protein Analysis Through Evolutionary Relationships

PBS – Phosphate buffer saline

PCA – Principal Component Analysis

PVDF - Polyvinylidene difluoride

RNA – Ribonucleic Acid

RNA-Seq – RNA Sequencing

SAM – Sequence Alignment/Map

SDS – Sodium dodecyl sulphate

ST – Steady state

TLR4 – Toll like receptor 4

UTR – Untranslated region

1. ABSTRACT

Dendritic cells (DCs) are key immune modulators and are able to mount immune responses or tolerance. DC differentiation and activation imply a plethora of molecular and cellular responses, including transcriptional changes. PU.1 is a highly expressed transcription factor in DCs and coordinates relevant aspects of DC biology. Due to their role as immune regulators, DCs pose as a promising immunotherapy tool. However, some of their functional features, such as survival, activation or migration, are compromised due to the limitations to simulate *in vitro* the physiological DC differentiation process. A better knowledge of transcriptional programs would allow the identification of potential targets for manipulation with the aim of obtaining “qualified” DCs for immunotherapy purposes. Most of the current knowledge regarding DC biology derives from studies using mouse models, which not always find a parallel in human. In the present study we dissect the PU.1 transcriptional regulome and interactome in mouse and human DCs, in the steady state (ST) or LPS-activated. The PU.1 transcriptional regulome was identified by performing PU.1 chromatin immunoprecipitation followed by high throughput sequencing and pairing these data with RNA-sequencing data. The PU.1 interactome was identified by performing PU.1 immunoprecipitation followed by mass spectrometry analysis. Our results portray PU.1 as a pivotal factor that plays an important role in the regulation of genes required for proper DC activation and function, and assures the repression of non-lineage genes. The interspecies differences between human and mouse

DCs are surprisingly substantial, highlighting the need to study the biology of human DCs.

2. INTRODUCTION

Dendritic cells (DCs) are key regulators of the immune system. They are able to mount an immune response or induce self-tolerance, by presenting antigens (or autoantigens) to specialized B and T cells. In homeostatic conditions (steady state), two major types of DCs can be defined in both human and mouse, namely plasmacytoid DCs (pDCs) and conventional DCs (cDCs). DC classification has gone through rapid updates in the past years and, currently, cDCs are subclassified as cDC1 ($CD141^+|XCR1^+$ in human and $CD8a^+$ in mouse) and cDC2 ($CD1c^+$ in human and Sirp-a^+ in mouse). Under inflammatory conditions, both in human and in mouse, a third type of so-called inflammatory DCs derives from circulating monocytes. Upon pathogen recognition, DCs become activated. This process includes secretion of cytokines as well as the upregulation of activation markers, such as MHC-II, CD40, CD86 and the C-C chemokine receptor 7 (CCR7).[1,2]

DC differentiation and activation is tightly regulated by transcriptional programs which are executed by transcription factor complexes.[3] One of these transcription factors is PU.1, encoded by the *Spi1* (mouse)/*SPI1* (human) gene, which belongs to the ETS-family of transcription factors.[4] PU.1 is important for the differentiation of hematopoietic myeloid lineages and for the proper differentiation and activation of DCs. Indeed, loss of PU.1 results in a general cDC reduction, which is dose-dependent, *e.g.* the lower the PU.1 expression, the more severe the reduction in cDC numbers. PU.1 is also involved in the lineage choice between cDC and pDC, being more prominently expressed in cDCs than in pDCs.[5]

PU.1 regulates the expression of CD80, CD86 and MHC-II by directly binding to the *GAGGAA* consensus sequence present on their promoter regions.[6,7] Furthermore, PU.1 is known to interact with several co-factors, which in turn modulate whether a PU.1 transcription complex will activate or repress transcription.[8-13] For example, PU.1 can form a complex with the coactivator c-Jun and enhance the expression of myeloid genes in macrophages. However, when c-Jun is replaced by GATA1 at those sites, as occurs in erythroid progenitors, the expression of myeloid genes is repressed.[14] A similar observation was done when PU.1 interacts with RUNX1, which results in displacement of co-repressors by co-activators at binding sites, thus promoting transcription.[15]

Due to their regulatory role in the immune response, methods to generate DC-based vaccines for immunotherapy purposes have been developed. The most common method is to generate monocyte- or $CD34^+$-derived inflammatory DCs, which will be activated and loaded with specific antigens *in vitro* prior to clinical application.[16] However, *in vitro* generated DCs differ substantially in quality and functional capacities from DC subsets isolated from blood or tissues. This difference accounts for sub-optimal immunotherapy efficacy.[17] Alternative methodologies to obtain “physiological” DC subsets are still under development. In fact, recent developments allow the use of primary or $CD34^+$ derived DC for immunotherapy purposes. However, these options are at an early stage and, though promising, are efficient only in limited clinical scenarios.[18-20] A recent method describes the generation of pDC, cDC1 and cDC2, in the presence of

stromal/feeder cells, which is a limitation for its use in the clinic.[21,22] The generation of human monocyte-derived inflammatory DCs (moDCs) requires both GM-CSF and IL-4, whereas mouse bone marrow-derived inflammatory DCs (BMDCs) are generated by GM-CSF alone.[23] This already portraits the interspecies differences. While in human IL-4 is required to prevent macrophage (MF) development in DC cultures,[24] in mouse BMDC cultures, addition of IL-4 results in pre-activated DCs that express higher levels of MHC-II, CD86 and CD40, rendering them anergic to further stimulus.[25]

Most studies on transcriptional regulation in DCs, and therefore studies on PU.1, have been performed in mouse models,[3] which still stand as a critical model system in the current knowledge of DC biology and function, as they allow the study of immune responses *in vivo*. However, caution should be taken when extrapolating results between species, as biological processes might not always be comparable. In the present study, the PU.1 transcriptional regulome (as identified by chromatin immunoprecipitation followed by high throughput sequencing – ChIP-Seq, paired with RNA-Seq data) and the PU.1 interactome (as identified by co-immunoprecipitation of PU.1 binding partners followed by mass spectrometry analysis) were analyzed and compared between human and mouse *in vitro* derived inflammatory DCs in the steady state (ST) or after LPS stimulation. PU.1 was found to regulate 770 genes both in human and mouse DCs in both unstimulated and LPS-stimulated cells, of which 582 genes are expressed in DC and 188 genes are not.

The PU.1 regulome displayed a great interspecies divergence, since a range of 20-35% (depending on species and expression/repression) of genes were regulated by PU.1 commonly in mouse and in human DCs. These core regulated genes are involved in cellular homeostasis and required for the immune specific functions of DCs, as extrapolated from GO Term enrichment analysis. Interestingly, many genes bound by PU.1 (ChIP-Seq) were not found to be expressed in DCs, suggesting a PU.1 transcription repression function, which indicates an important role in lineage specification. Lastly, PU.1 interacting co-factors were identified, and similar interspecies divergence was observed. A model of PU.1 transcription factor complex and core transcriptome in unstimulated and LPS-stimulated human and mouse DCs is proposed.

Since DCs are a promising tool for immunotherapy in human, it is important to study transcriptional program changes in human DCs in more depth, and to understand how interchangeable the two model systems are. We suggest that this sort of analyses, aimed at basic knowledge generation, will allow to develop strategies for DC manipulation in order to generate more efficient DCs for immunotherapy purposes in the future, and to understand the crossroads of the innate and adaptive immune response in pathologies characterized by (chronic) inflammation.

3. METHODS

3.1. Human monocyte-derived dendritic cell (moDC) culture

Human monocyte-derived dendritic cells (moDCs) were cultured as described before.[25] Informed consent was obtained as approved by our institute medical ethics committee and in accordance with the 1964 Declaration of Helsinki. In short, monocytes were isolated with $CD14^+$ magnetic beads (Miltenyi Biotech, Bergisch Gladbach, Germany) from the PBMC fraction of the blood from healthy donors and $0.5x10^6$ monocytes mL^{-1} were seeded. Alternatively, monocytes were enriched based on plastic adhesion. In brief, 150×10^6 PBMC were seeded into T75 cell culture flasks and allowed to adhere in a 5% CO2 incubator at 37°C for 1 hour in 15 ml of RPMI-1640 supplemented with 10% FCS, 1% Penicillin and Streptomycin (all from Life Technologies, Carlsbad, CA, USA). Non-adherent cells were removed after carefully washing the adherent monocytes with PBS prior addition of conditioned culture medium. Monocytes were cultured for 7 days in RPMI-1640 supplemented with 10% FCS, 1% Penicillin and Streptomycin, 10 ng mL^{-1} GM-CSF and 10 ng mL^{-1} IL-4 (both Peprotech, Rocky Hill, NJ, USA) after which half of the cells were stimulated with 500 ng mL^{-1} LPS (Santa Cruz Biotechnology, Dallas, TX, USA) and the cells were harvested at day 10.

3.2. Mouse bone marrow-derived dendritic cell (BMDC) culture

Bone marrow cells were isolated from C57Bl/6 mice, containing a reporter gene under the CD11c promoter (R26R-RG|CD11cCre) and cultured as described before.[25] In short, bone marrow cells were isolated from the femora and tibiae by

crushing the bones and filtering the cell suspension through a cell strainer. $0.5x10^6$ cells mL^{-1} were cultured for 7 days in RPMI-1640, supplemented with 5% FCS, 1% Penicillin/Streptomycin (all from Life Technologies, CA, USA), 5 µM 2-mercaptoethanol (Sigma-Aldrich, St. Louis, MO, USA) and 20 ng mL^{-1} GM-CSF (Peprotech, Rocky Hill, NJ, USA) after which half of the cells were stimulated with 500 ng mL^{-1} LPS (Santa Cruz Biotechnology, Dallas, TX, USA) and were harvested on day 10, after which the reporter positive cells ($CD11c^+$ cells, e.g. DCs) were sorted.

All mice were kept under specific pathogen-free conditions with free access to food and water, under the guidelines for animal experimentation approved by the Animal Ethical Committee (nr. 10.018).

3.3. Chromatin immunoprecipitation and sequencing (ChIP-Seq)

Chromatin immunoprecipitation (ChIP) was performed as described by Follows *et al.*[26] In short, after cross-linking the chromatin of $2x10^8$ moDCs (from two independent donors) or BMDCs (from two independent mice) was sonicated into fragments of approximately 200 bp. PU.1 (T-21, Santa Cruz) and rabbit IgG (Invitrogen, Carlsbad, CA, USA) antibodies were used for immunoprecipitation. After elution of the antibody and digestion of the proteins, the DNA was sequenced using the Illumina GAIIx sequencer as described previously by Soler *et al.*[27] Data is deposited in Genbank with ID number GSE123347.

3.3.1. Data analysis

Raw reads were mapped to version mm9 of the *Mus musculus* genome (BMDCs) or to version GRCh37 (hg19) of the *Homo sapiens* genome (moDCs) using bowtie.[28] After mapping, reads were sorted and converted from Sequence Alignment/Map (SAM) to Binary Alignment/Map (BAM) format using SAMtools.[29] Peak identification of binding sites of PU.1 was done using the MACS program (v1.4.1),[30] with the following settings: bandwidth 125 and a lower and upper M-fold cutoff of 8 and 30 respectively. The reads obtained from the two independent experiments were merged for analysis. Enriched motifs within the peak regions were determined using the MEME program (v4.9.0).[31]

Genes regulated by these binding sites were predicted using the 'refgene_getnearestgene' tool from CisGenome[32] in combination with the 'mm9_refFlat_sorted.txt' gene annotation file (BMDCs) or "refFlat_sorted(hg19).txt" (moDCs), downloaded from the CisGenome website. Peaks were associated with differentially expressed genes, and differential motif enrichment was determined using Binding and expression target analysis (BETA).[33] Peaks associated with differentially regulated genes were also analyzed for motif enrichment using Hypergeometric Optimization of Motif EnRichment (HOMER).[34]

3.4. RNA Sequencing (RNA-Seq)

3.4.1. MOUSE BMDC

We used RNA-Seq data previously generated by us (GSE69969).[35] We trimmed off adapter sequences and mapped the trimmed reads against the requested

reference (GRCm38.p4) using HiSat2 (version 2.1.0). We called gene expression values using HTseq-count (version 0.11.2).

3.4.2. HUMAN moDC

RNA was isolated from human moDC, stimulated or not with LPS (from two independent donors) following standard procedures, using a Trizol-based extraction method. RNA samples were prepped with the Illumina TruSeq Stranded mRNA Library Prep Kit and sequenced according to the Illumina TruSeq Rapid v2 protocol on an Illumina HiSeq2500 sequencer. Reads were generated of 50 bp in length. We trimmed off adapter sequences and mapped the trimmed reads against the requested reference (GRCh38.p5) using HiSat2 (version 2.1.0) We called gene expression values using HTseq-count (version 0.11.2). The data were submitted to GEO (accession number GSE157844).

3.4.3. Data analysis

Differential gene expression analysis was performed within the R environment (version 3.6.0), with the edgeR package. The raw read counts per transcript were normalized by library size and by differences in sequencing depth between samples using the trimmed mean of M-values (TMM) method, but they were not adjusted by gene length. A threshold of at least 30 counts per million reads in at least one group (min.count = 30) was set to remove low-expressed genes. Common and tagwise dispersions were estimated by the quantile-adjusted conditional maximum likelihood (qCML), and differential expression of transcripts

was assessed with the 'exactTest' function, based on the qCML methods. False discovery rate (FDR) control was used to correct for multiple testing, and an adjusted P value of < 0.05 was considered significant.

3.5. Immunoprecipitation (IP)

3.5.1. Protein isolation and PU.1 IP

Approximately $4x10^7$ cells were lysed in 1 mL of RIPA Buffer (10mM Tris-HCL pH 8, 1mM EDTA, 0.5 mM EGTA, 140 mM NaCl, 1% TritonX100, 0.1% NaDOC, 0.1% SDS) with fresh protease inhibitors (Roche, Basel, Switzerland). Protein concentrations were measured with BCA Protein Assay Reagent (Thermo Fisher Scientific, Rockford, IL, USA). 500 μg of lysate was used per IP. First, lysates were pre-cleared with 50 μl Dynabeads Protein A that had been previously washed with PBS and equilibrated in RIPA buffer. 10 μl Anti-PU.1 (T-21, Santa Cruz) antibody was added, and samples were incubated for 16 hours at 4°C with rotation. After this, 50 μl of washed and equilibrated Dynabeads Protein A was added and left incubating for an extra hour at room temperature (RT) with rotation. Dynabeads were collected by placing the tubes on a magnet holder and resuspended in 100 μl PBS for further processing. As IP antibody control, we used Rabbit IgG (Invitrogen).

3.5.2. In-solution digestion for mass spectrometry analysis

Samples were digested for 16 hours at 37°C with MS-grade trypsin (Promega, Fitchburg, WI, USA) in a ratio of 1:20 trypsin:protein to a maximum of 1.2 μg

Trypsin after standard disulfide bond reduction and alkylation procedure. Tryptic peptides were desalted and concentrated using 3M Empore-C18 StageTips (Sigma-Aldrich, St. Louis, MO, USA) that were made following a described procedure[36] and eluted with 0.5% (v/v) acetic acid (Sigma-Aldrich), 80% (v/v) acetonitrile (acetonitrile and water are from Biosolve Chimie, Dieuze, France). Sample volume was reduced by SpeedVac and supplemented with 2% acetonitrile, 0.1% trifluoroacetic acid (TFA) (Thermo Fisher Scientific) to a final volume of 7 µl, of which 2 µl was injected for MS analysis.

3.5.3. Mass spectrometry analysis

Tryptic peptides were separated by nanoscale C18 reverse phase chromatography coupled on line to an Orbitrap Fusion Tribrid mass spectrometer (Thermo Fisher Scientific) via a nanoelectrospray ion source (Nanospray Flex Ion Source, Thermo Fisher Scientific), following standard procedures and settings. All data were acquired with Xcalibur software.

3.5.4. Proteomics data analysis

The raw mass spectrometry data were analyzed with MaxQuant software version 1.5.5.1 using default settings and Label Free Quantification (LFQ). Data is deposited in Proteome Exchange with ID numbers PXD011903 (human) and PXD011904 (mouse). The peptides were identified searching against the UniProt KB human or mouse taxonomy database.[37-39]

The output Protein Groups table generated by MaxQuant was used as input for Perseus software paired version for further analysis. Reverse hits and potential contaminants were removed. A generalized logarithm transformation [$\log_2(x)$] was applied to all Label Free Quantification (LFQ) intensity values to stabilize the variance across the full intensity range. We removed background/unspecific bound proteins when identified in IgG IP controls. Log2LFQ values from LPS or ST samples were merged from the two independent samples per condition. The Log2 ratio LPS vs ST was calculated. The filtered lists of identified proteins were used for further analysis as indicated below.

3.6. Western blotting

Western blotting was done as described.[25] Briefly, protein extracts from the input material, immunoprecipitate and supernatant fractions were separated on a 10 or 12.5% SDS-polyacrylamide gel and transferred to a PVDF (Millipore, Billerica, MA, USA) membrane. The membranes were incubated with a rabbit polyclonal PU.1 antibody (T-21, Santa Cruz) or mouse monoclonal STAT5B antibody (G-2, Santa Cruz), using an HRP-conjugated anti-rabbit or anti-mouse IgG as secondary antibody, respectively. Amersham ECL Prime Western blotting detection reagent (GE Healthcare) was used on membranes, which were developed using a Li-Cor Odyssey Fc device.

3.7. Further data analysis

Mouse to Human ortholog gene lists were obtained using the gprofiler2 R package (version 0.2.0).

Mouse to Human ortholog gene lists were obtained using Ensembl/BIOMART, release 94.[40] Upstream regulators were identified using TRRUST v2.[41] Kyoto Encyclopedia of Genes and Genomes (KEGG) enrichment on gene lists were obtained using the goseq (version 1.36.0), and the msigdbr (version 7.0.1) R packages. Length bias was not taken into account, due to the double origin of the gene list, and the enrichment was calculated with the hypergeometric method. The resulting P values were adjusted for multiple testing using the Benjamini and Hochberg correction, and an adjusted P value of < 0.05 was considered significant. Protein-protein interaction graphics were obtained using STRING database.[42] Identification of transcription regulators in gene lists was done using Protein Analysis Through Evolutionary Relationships (PANTHER) version 14.[43] Venn diagrams were built using a web-based tool from the VIB / UGent Bioinformatics & Evolutionary Genomics Group (http://bioinformatics.psb.ugent.be/webtools/Venn/) and Euler diagrams were built using R or the web-based tool Meta-chart (https://www.meta-chart.com/venn).

4. RESULTS

4.1. Culture and stimulation of human and mouse inflammatory DCs

The monocyte-derived DC (moDC) culture method is currently the most widely used for the generation of DCs for immunotherapy purposes,[16] despite this method generates inflammatory DC which differ from steady state DC. However, most studies on the quality and functional capacity of DCs have been performed in mouse models.[3,44] In order to bridge the current study models at the molecular level we designed an interspecies study based on this *in vitro* model, where we aimed at the identification of the PU.1 transcriptome and interactome in human and mouse inflammatory DCs, stimulated or not with a TLR4 agonist (LPS) (Fig. 1A). The time points selected during DC culture and upon LPS stimulation were chosen based on previous studies, where a significant downregulation of PU.1 in mouse BMDC cultures was observed 72hr upon LPS stimulation.[45] LPS stimulation resulted in activated or mature DCs in both culture systems, as extrapolated from the upregulation of the co-activation marker CD86 (Fig. 1B).

Culture of human moDCs requires the addition of GM-CSF and IL-4 to the cultures, as GM-CSF alone drives the monocytes to differentiate into macrophages.[24] However, mouse BMDCs which are phenotypically equivalent to human moDCs are cultured from bone marrow progenitors using GM-CSF only. Addition of IL-4 to mouse BMDC cultures generates pre-stimulated DCs which are anergic to further stimulus.[25] A recent report suggested that mouse BMDCs generated with GM-CSF are a heteregeneous culture that may contain up to 40% of macrophages (MF).[23] Concerned by this, we analysed by flow cytometry our

cultures, and identified residual MF presence (Fig. 1B). Comparison of RNA-Seq from our DC cultures with publicly available data on mouse tissue isolated cell types showed that our BMDC cultures cluster together with DCs but not with MFs, supporting the notion that the residual MF presence confers undetectable interference at the transcriptome level in mouse BMDC.[35] In addition, we performed comparison of RNA-Seq from our human DC cultures with publicly available data on human prospectively isolated DC and other primary hematopoietic non-DC cell types, showing that human moDC cluster close to primary DC and appart from non-DC cell types (Supplementary Figure 1). We therefore are confident that we were able to generate through this culture method enough numbers of inflammatory DC, from mouse and human culture systems, and decided to rely on these models for further analysis.

4.2. Characterization of PU.1 binding sites and consensus sequence in mouse BMDCs

In order to get insight into PU.1 transcriptional targets in mouse BMDC and how they might shift upon immunogenic stimuli, we performed PU.1 chromatin immunoprecipitation followed by high throughput sequencing (ChIP-Seq) on mouse unstimulated or LPS-stimulated BMDC, from two independent cultures. Peak calling of sequence reads was performed, after merging data from samples of the same condition, using MACS normalization.

We identified a larger number of peaks unique to ST mouse BMDCs (55,493) than peaks unique to LPS-stimulated BMDCs (19,916), which supports the trend

of PU.1 protein expression downregulation identified previously on GM-CSF BMDC upon LPS stimulation.[45] PU.1 ChIP-Seq revealed 46,326 peaks common to both ST and LPS-stimulated DC (Fig. 2A). Using MEME analysis, we identified the TTCCtc motif (reverse complementary to gaGGAA) in ST BMDC samples, whereas the GaGGAA motif was enriched in samples from LPS-stimulated BMDC (Fig. 2A). This validates the PU.1 ChIP-Seq quality and specificity, as the already known PU.1 binding site is enriched in our experiments. 65-75% of the peaks were found on intronic or intergenic locations. 10-15% of the peaks were located upstream regulatory regions (promoter and enhancers) and 10% on downstream regulatory regions (enhancers). 4.5-7.5% of the peaks were found on an untranslated region (UTR) or on a coding sequence (CDS) (Fig. 2B). The enrichment of the peaks on known promoter sites or bidirectional promoter sites of maximum 5,000 bp upstream of a gene was analyzed. Both unidirectional and bidirectional promoter sites were highly enriched in both conditions (Fig. 2C).

2,931 genes were assigned to the identified peaks in ST BMDC, whereas 3,518 genes were assigned to be putatively regulated by PU.1 in LPS-stimulated BMDCs (Supplementary Table 1, Supplementary Dataset 1A and GSE123347), supporting previous reports.[46] Although levels of PU.1 in mouse BMDCs strongly decreased upon LPS stimulation,[25,45] as well as the number of identified peaks in PU.1 ChIP-Seq analysis, the number of assigned regulated genes by PU.1 in mouse BMDCs slightly increased upon LPS stimulation.

In order to get insight into active transcription or repression of PU.1 putatively regulated genes, ChIP-Seq data was overlaid with RNA-Seq data from GM-CSF

BMDC cultures stimulated or not with LPS,[35] as described in the Methods section. This analysis showed that approximately 28% of DC expressed genes are positively regulated by PU.1 either in ST or LPS-stimulated cells or in both conditions. Interestingly, this analysis showed that approximately 35% of assigned PU.1 putatively regulated genes as extrapolated from our ChIP-Seq datasets -on either condition- were not expressed in DCs, suggesting that PU.1 might actively repress the expression of those genes in BMDC (Fig. 2D, Supplementary Table 1 and Supplementary Dataset 1A).

We next selected differentially expressed genes that were either up- or downregulated in DCs upon LPS stimulation in our culture system (approximately 10% of the expressed genes) and paired these with the PU.1 ChIP-Seq datasets as to assign activating or repressing functions of PU.1 upon LPS stimulation. This analysis showed that around 25% of the differentially expressed up- or downregulated genes upon LPS stimulation were regulated by PU.1 (Fig. 2E, Supplementary Table 1 and Supplementary Dataset 1A).

KEGG pathway analysis and GoTerm Enrichment analysis was applied to dissected subgroups of PU.1 regulated genes in order to get insight on cellular processes, highlighting the prevalence of immune-related responses, metabolism and signaling on expressed genes (data not shown and Supplementary Dataset 1B). Interestingly, the list of genes repressed by PU.1 in BMDC, *i.e.* identified in our ChIP-Seq data but not expressed in BMDC RNA-Seq data, was enriched for cardiac and neurologic pathways (*i.e.* repressed genes were enriched for non-DC or non-immune pathways).

4.3. Characterization of PU.1 binding sites and consensus sequence in human moDCs

We next set out to perform the same parallel analysis on human moDC either LPS-stimulated or not. All significantly enriched peaks found in unstimulated and LPS-stimulated samples were compared. 3,101 peaks were found uniquely in unstimulated moDC samples, whereas 85,729 peaks were found solely in LPS-stimulated samples. 6,751 peaks were found common to both conditions (Fig. 3A).

Using MEME analysis the PU.1 known consensus sequence (gaGGAA) was identified in both conditions, indicating a preferential direct binding of PU.1 to the DNA on target genes in moDCs, and validating the quality and specificity of our dataset (Fig. 3A). Subsequently, the specific locations of the peaks in the genome were analyzed. Most of the peaks, about 75-80%, were intronic or intergenic. Around 10% of the peaks were located on upstream regulatory sequences, and slightly less (8-9%) on downstream regulatory sequences. Only 2% of all identified peaks were found either on an UTR or on a CDS (Fig. 3B). The enrichment of the peaks on known promoter sites or bidirectional promoter sites of maximum 5,000 bp upstream of a gene was analyzed. In ST moDCs, all promoter sites (1,000, 2,000, and 3,000 bp upstream of a gene) were found to be significantly enriched in the ChIP-Seq samples compared to the genome, however, PU.1 did not bind any bidirectional promoters. Upon LPS stimulation, all promoter sites were highly enriched compared to the genome, including

bidirectional promoters (Fig. 3C). This differs from murine BMDCs, where PU.1 binds to bidirectional promoters both in the ST and upon LPS stimulation. Next, the identified peaks were assigned to putatively regulated genes as described, which resulted on a similar number of genes in the ST (1,577) and LPS stimulated condition (1,519) (Supplementary Table 1 and Supplementary Dataset 2A).

In order to get insight into active transcription or repression of putatively regulated genes, ChIP-Seq data was combined RNA-Seq data from moDC cultures, stimulated or not with LPS, as described in the Methods section. This analysis showed that approximately 15% of DC expressed genes are positively regulated by PU.1 in either ST or LPS-stimulated condition or both. It also showed that either in ST or LPS-stimulated conditions approximately 30% of assigned PU.1 ChIP-Seq genes were not expressed in DCs, suggesting that the repressive role of PU.1 in human DC is rather crucial, and maintained as compared to mouse inflammatory DC (Fig. 3D, Supplementary Table 1 and Supplementary Dataset 2A).

The significantly differentially expressed genes upon LPS stimulation were stratified based on up- or downregulation (approximately 30% of the expressed genes) and overlaid with the PU.1 ChIP-Seq datasets as to assign potential activating or repressing functions of PU.1 due to moDC LPS stimulation. This analysis showed that 20% of the up- or downregulated genes were actively regulated by PU.1 upon LPS stimulation (Fig. 3E; Supplementary Table 1 and Supplementary Dataset 2A).

KEGG pathway analysis and GoTerm Enrichment analysis was applied to dissected subgroups in order to get insight on cellular processes, highlighting the prevalence of immune-related responses, metabolism and signaling as observed with mouse DC datasets (data not shown and Supplementary Dataset 2B). In human moDC, we identified additional evidence that the PU.1 repressive function might be very relevant in this cell type, as KEGG enrichment was significant on the subset of genes that are upregulated upon LPS activation, but that are repressed by PU.1 at the ST condition (*i.e.* upon LPS stimulation, PU.1 is released from the chromatin at those gene-locations). In this subset, the three key aspects of DC performance appear: migration, survival and immune activation. Similar to the mouse analyses, genes putatively regulated by PU.1, but not expressed in DC (*i.e.* repressed by PU.1), enriched for neurologic pathways and signaling pathways relevant in other immune cells.

4.4. Comparison of PU.1 regulated genes in mouse and human DCs

We next set out to bridge the identified transcriptome and its dynamics between human and mouse inflammatory DCs. The Human and Mouse Orthologous Gene Nomenclature (HUMOT) was used using edgeR platform to directly compare PU.1-regulated genes in human and mouse DCs. This conversion resulted in a 13% loss of genes because some orthologs could not be assigned due to paralogues or duplication of genes. The human ortholog list was obtained from the mouse gene lists employed as described above, and *vice versa* (Fig. 4A). For the definitive comparison interspecies, we overlaid the human datasets with the

mouse-to-human ortholog translation datasets sharing the same dynamics regarding condition (ST or LPS stimulated condition or both) and expression profile (differentially expressed or not in DCs and up- or downregulated) (Fig. 4, Supplementary Tables 1-2 and Supplementary Dataset 3).

The overlay of assigned genes through ChIP-Seq analysis resulted in a partial conservation of dynamics interspecies, shortlisting only 58 common genes regulated by PU.1 in ST condition, 84 genes in LPS stimulated condition and 185 genes in both (Figs. 4A,C). When comparing genes expressed in DCs, 9,158 genes were commonly expressed in mouse and human DC (Fig. 4B). The overlay of the common expressed genes (RNA-Seq) and those regulated by PU.1 (ChIP-Seq) of human and mouse DCs, resulted in 188 common genes that are not expressed in DC but are repressed by PU.1 in both species (Fig. 4D, Supplementary Tables 1-2 and Supplementary Dataset 3A). When analyzing up- or downregulation upon LPS stimulation, 122 genes were commonly upregulated and 179 genes were commonly downregulated (Figs. 4B,E; Supplementary Table 1 and Supplementary Dataset 3A). Supplementary Table 1 shows that the subset of genes that are not expressed in DCs and are repressed by PU.1 are the ones with more common interspecies hits, while the ones of which the expression is up- or down regulated upon LPS stimulation diverge largely.

KEGG pathway and GoTerm Enrichment analyses highlighted the conservation of the PU.1 regulome related to genes involved in signaling (Supplementary Table 2 and Supplementary Dataset 3B). Interestingly, KEGG and GO Term enrichment revealed neurologic, cardiac and signaling pathways in the non-DC

genes repressed by PU.1, supporting the notion that the repressive gene expression function of PU.1 is a relevant transcription regulation feature of PU.1 in DCs, and is conserved interspecies.

4.5. Characterization of PU.1 binding partners in human and mouse DCs

PU.1 forms part of transcription factor complexes, which depending on their nature will participate in positive or negative transcription regulation. Combining the ChIP-Seq analysis with available RNA-Seq datasets potential repressing or activating functions of PU.1 in the transcription dynamics of sets of genes upon LPS stimulation of DCs could be assigned. In order to get insight on relevant binding partners of PU.1 in human and/or mouse DCs, the interactome was dissected at whole cell level on human and mouse inflammatory DCs both in ST and LPS stimulated condition.

PU.1 co-immunoprecipitation (co-IP) and identification of binding partners by mass spectrometry was performed as described. In Fig. 5A, Principal Component Analyses (PCAs) of respective PU.1-co-IP in mouse and human inflammatory DCs are depicted. PU.1 co-IP clustered separated from IgG-coIP controls, although, this separation was more robust in human samples than in mouse samples. Similarly, PU.1 co-IP in ST condition clustered separated from LPS-stimulated DCs, indicating qualitative and quantitative changes in the PU.1 interactome upon LPS stimulation. Of note, the separation amongst conditions was again more robust for the human samples. As technical validation of our pull-down experiments, we were able to identify SPI1 (PU.1) in all PU.1 co-IP

samples, *i.e.* human and mouse samples both ST and LPS stimulated condition (Supplementary Dataset 4). As proof of principle, western blot analysis of pull-downs performed in mouse BMDC and human moDC cultures stimulated or not with LPS (Fig. 5B), showed PU.1 detection and STAT5B on respective co-IPs.

We identified 1,165 proteins to co-IP with PU.1 in mouse BMDCs in ST condition and 957 proteins in LPS-stimulated BMDC (Fig. 5C, PXD011904 and Supplementary Dataset 4A). Selecting only the nuclear proteins reduced the list to 452 and 388 interacting proteins in ST or LPS stimulated condition respectively (Fig. 5C). Of these nuclear proteins, the transcription regulators are identified using PANTHER platform (Fig. 6A), showing that the core interactome includes STAT1, STAT5B, REL and IRF5. Chromatin remodeling factors such as HMGB1 or SMARCC1 are part of the interactome in ST condition, whereas NFKB1 and NFKB2 are part of the PU.1 interactome upon LPS stimulation (Fig. 6A and Supplementary Dataset 4A). The schematic representation shows that PU.1 co-factors include transcription factors that have been described as repressors, as well as other proteins involved in RNA processing and turnover (Fig. 6A).

In the PU.1 co-IP samples from human moDCs, we identified 1,207 interacting proteins in ST and 1,286 interacting proteins in LPS stimulated condition (Fig. 5C, PXD011903 and Supplementary Dataset 4B). Filtering for only nuclear proteins reduced the list to 501 and 562 interacting proteins in ST and LPS stimulated condition, respectively. The curated nuclear transcription regulators (Fig. 6B) highlights a core interactome formed by STAT1, STAT5B, PML and HMGB1, as

well as interacting partners that are unique for ST or LPS stimulated condition. The interactome in ST condition is residual, including several transcription repressors, while a number of relevant transcription factors are identified in LPS condition, such as NFKB1 and NFKB2, REL, RELA, IRF5, and other STATs (Fig. 6B).

Overlaying the PU.1 interactome after obtaining the human ortholog translation from mouse datasets (Fig. 5D, Supplementary Table 3) resulted in a core interactome, that is maintained in inflammatory DCs regardless of their activation status, the interactome in unstimulated DCs and the interactome of LPS stimulated DCs.

KEGG pathway analysis of the core interactome and interacting partners during ST conditions pointed to RNA metabolism (splicing, processing). PU.1 is known to bind RNA and to play a role in the splicing process,[47] which may explain the presence of ribosomal proteins, chaperonins and other translation related proteins identified by mass spectrometry in our samples. In contrast, the enriched KEGG pathways of LPS stimulated samples did relate to the innate immune response, supporting the notion that rearrangement of PU.1 transcription factor complexes upon LPS stimulation serves immune response related cellular functions (data not shown and Fig. 6B).

4.6. Interspecies model of the PU.1 interactome and transcriptome

In order to design an overview of the dynamics of PU.1 interacting proteins upon LPS stimulation and its impact on the PU.1 transcriptome in human and mouse

DCs, the upstream regulators from the shortlisted set of genes regulated by PU.1 (ChIP-Seq and RNA-Seq, common interspecies) were overlaid with the identified proteins in our pull-down assays, allowing to draw a simplified model of PU.1 complex formation in both species (Supplementary Figure 2). The pathway enrichment of common target genes was incorporated to this model in order to visualize the PU.1 driven processes in inflammatory DC.

The filtered interactome interspecies showed common binding partners (STATs, NFKBs, FLII) in similar conditions (*i.e.* ST or LPS-stimulated). Other PU.1 partners, including chromatin remodeling factors like HDAC1 (mouse), are recruited to PU.1 in the ST condition.

KEGG pathway and GoTerm enrichment analysis of the PU.1-regulated but not expressed genes common interspecies (*i.e.* repressed genes) resulted in non-DC and non-immune pathways, while KEGG pathway enrichment of DC-expressed genes regulated by PU.1 common interspecies resulted in signaling pathways, amongst others. This model highlights the common features between human and mouse inflammatory DCs, however, it is a limited view of the whole scenario, and portrays the divergence of the nature of inflammatory DCs interspecies (and potential culture-method related differences), despite functional and immune-phenotypical (expression of surface markers) similarities.

Overall, this analysis emphasizes the difficulty to translate results found in the murine model system to human cells. Although an overlap between human and mouse DCs was found, we were unable to identify or predict a core PU.1 transcription factor complex shared interspecies. This study did identify several

new cofactors for PU.1 in human moDCs, and several common target genes and pathways, which should be further studied as possible candidates for manipulation and improvement of DC function when used as immunotherapy tool, and to better understand the basis and crossroads between innate and adaptive immune responses in pathologies with subjacent inflammation.

5. DISCUSSION

In this study, the transcriptome and interactome of PU.1 was compared between human and mouse inflammatory DCs generated by culturing peripheral blood monocytes or bone marrow precursors, respectively. This was done in order to compare interspecies the final product of an analogue DC type, *i.e.* in this case inflammatory, being the major type used in order to generate and prime DC prior immunotherapy, although new strategies are being implemented which use primary or $CD34^+$ derived DC.[18-20] The flaws of the system have largely been discussed in the literature. GM-CSF/IL-4 derived moDC are far from resembling DC subtypes identified *in vivo*, and their properties are probably not the finest for each specific immunotherapeutic purpose. However, the generation of conventional DCs in culture, or maintenance, is a limiting factor.

As mentioned before, the culture requirements for the generation of mouse or human DCs already portray that the two systems are essentially different. Furthermore, despite PU.1 being an essential factor in mouse and human DCs, as we described previously, the dynamics of PU.1 expression in DCs upon LPS stimulation is different interspecies. In human moDCs, the expression of PU.1 increases about 3-fold upon LPS activation, whereas it decreases about 10-fold in mouse BMDCs. These findings support the power of identified peaks from our ChIP-Seq data sets. However, the number of PU.1-regulated genes predicted from the peak-calling did not correlate with more or less expression of PU.1. In addition, about 3-fold more genes were predicted to be regulated in mouse DCs compared to human DCs. This suggests that PU.1 binds multiple promoter and

enhancer sites per regulated gene. Of note, the predictions derived from ChIP-Seq analyses do not give information on whether the expression of a given gene is being activated or repressed. For that reason, we paired our ChIP-Seq datasets with RNA-Seq data.

Indeed, from this pairing we could observe that about 30% of genes putatively regulated by PU.1 are not expressed in DC in mouse and human respectively. This is an important proportion, and suggests that PU.1 is a crucial factor to contain or skew lineage commitment and differentiation, as KEGG pathway and GoTerm enrichment of PU.1 repressed genes on inflammatory DCs highlighted processes such as nervous or cardiac system development.

In unstimulated DCs, the common PU.1-regulated genes were involved in general cell functions, like nutrient sensing, lipid metabolism and energy production, which indicates the crucial function of PU.1 in DC biology (data not shown). The core PU.1-regulated genes found both in human and mouse DCs and both in unstimulated or LPS-stimulated DCs, included general genes, like several phospholipases, protein kinase C subunits, MAP kinases, calcium voltage channels, as well as genes important for the immune function of DCs, like *IL-4R, JAK1, mTOR*, and *TLR4*.

PU.1 has been reported to bind the proximal *CD11c* promoter directly.[48] We did not find the *ITGAX* gene encoding CD11c to be regulated similarly in our dataset. On the other hand, we did confirm previous findings that PU.1 binds directly to the promoter region of *CD80, CD86*,[6] and *CIITA* (MHC-II),[7] although not always following the same dynamics when comparing mouse and human DCs. From the

strict overlay performed with the common genes that follow the same dynamics between mouse and human (same signature on PU.1 binding in ST, LPS conditions or both, and same signature in the RNA-Seq, expressed, up- or downregulated or not expressed) we shortlisted a transcriptome that revealed PU.1 as a master regulator of lineage specification (repressing non-DC genes), and that PU.1 seems to be required for the activation of genes involved in DC relevant processes, including genes involved in signaling (related to PI3-Akt, MAPK and GTPases).

To further identify PU.1 transcriptional complexes in DCs we employed co-immunoprecipitation followed by mass spectrometry analyses. The number of transcription regulatory cofactors of PU.1 differed between human and mouse DCs. Interestingly, based on common and uniquely co-IPed proteins comparing DCs before and after stimulation, it looks as if in human DC, new partnerships are made upon LPS stimulation, while in mouse DCs, LPS stimulation triggers not only the formation of new partnerships, but also the loss of partnership required for DC to remain quiescent or unstimulated. This data is supported by the observation that PU.1 levels generally decrease in mouse BMDCs upon LPS stimulation.[25]

Several of the identified cofactors were previously described or suggested in the literature: *i.e.* STAT1,[8] STAT5A and STAT5B,[10] IRF4,[9] REL,[13] and NF-κB.[12] In addition, many cytoplasmic proteins were found in the IP samples. Since PU.1 is known to bind RNA and to play a role in the splicing process,[47] this may explain

the presence of ribosomal proteins, chaperonins and other translation related proteins identified by mass spectrometry in our samples.

We are aware that overlaying only the datasets behaving with the same pattern characteristics (*i.e.* genes bound by PU.1 in ST or LPS condition, expressed genes, up- or downregulated genes) results in loss of information, as many target genes and interacting proteins identified are present interspecies, however, they do not share interspecies the same compartmentalization.

Despite the limitations of the comparison performed, we were able to observe important aspects: PU.1 interacts with transcription regulators, but also with proteins which function in chromatin remodeling, RNA processing, chaperonins, protein degradation and signaling. When focusing on its interactions with nuclear transcription regulators, it was common to both species the presence of chromatin remodeler partners in the ST condition, and the replacement of these by transcription factors in the LPS condition. This suggests a pivotal function of PU.1 in DC gene expression regulation upon LPS stimulation. Furthermore, it was evident through our analysis that repression of gene expression by PU.1 is very relevant, as many genes (non-DC, non-immune) are putatively repressed by PU.1, making it an important factor in lineage specification.

In order to extract potential pathways or functions to manipulate or to tailor DCs for immunotherapy, the interspecies analysis may be very useful. It has been reported that mTOR inhibitors improve DC function and survival,[49] which supports the notion that PI3-Akt signaling fine tuning is required for DC immune activation and response to a triggering stimulus. Since this pathway enriched by

a subset of genes commonly regulated by PU.1 in human and mouse inflammatory DCs, it is worth exploring whether mTOR inhibition at a given stage during DC generation or priming would result in more competent DCs for immunotherapy. On the other hand, this might be a target to palliate inflammatory pathologies.

Very importantly, in human, we observed that PU.1 repressed a subset of genes in ST condition that are upregulated upon LPS stimulation. This subset of genes enriches for pathways related to survival, migration and activation. Manipulation of PU.1 levels might not be an appropriate strategy to generate tailored DCs, as it compromises their survival (loss of function). However, other identified partners or targets could be manipulated genetically or pharmacologically. HDACs are required for DC biology, and it has been shown that HDAC inhibitors alter the DC transcriptome, including PU.1 levels and PU.1 chromatin binding.[50] Exploration of HDAC inhibitor effects in human moDC appears as a potential strategy in order to manipulate PU.1 levels, especially when applying inhibitors at a given stage of differentiation or together with a priming stimulus.

Taken together, we improved the knowledge of the PU.1 interactome and transcriptome in DCs by identifying similarities and differences between human and mouse DCs, which is in line with recent reports and efforts trying to characterize the plethora of DC subsets.[17] PU.1 itself has been reported as a highly important transcription factor in both human and mouse DCs. It regulates many genes important for the maintenance of the cell, like lipid metabolism and energy production, as well as for the immune response. As extrapolated from our

data, it also has an important funcion as a gene expression repressor, probably necessary during lineage specification. From the interactome data, we also highlight the potential important role of PU.1 in RNA metabolism. As reported in mouse models, engineered loss of function of PU.1 will most likely result in lack of development and dysfunction of DCs. It might be effective to manipulate a cofactor of PU.1 to obtain less dramatic and possibly more specific changes in DC function without affecting DC development and integrity, or to enforce PU.1 activity at different levels. Importantly, in this manuscript we have dissected PU.1 regulatory features in DCs, while many other transcription factors govern DC biology. Manipulation of dissected cofactors or characterized pathways (pharmacologically) might increase the survival of DCs to improve efficacy of DC therapy, or will aid at the amelioration of pathologies with subjacent inflammation.

6. AUTHORSHIP

MRS performed experiments, analyzed data and wrote the manuscript; PMB analyzed data and wrote the manuscript; PdB, BN, ER, JAAD and RWWB analyzed data; NC-S, IMDC, VS and NG performed experiments; AMW, LvdL, WFJvI and AAH performed experiments and revised the manuscript; TKvdB, SP and TWK participated in discussions and revised the manuscript; LG designed experiments, analyzed data and wrote the manuscript.

7. ACKNOWLEDGEMENTS

This work was supported by a VENI grant from the Netherlands Scientific Organization (NWO; VENI 863.09.012) and a RYC fellowship from the Spanish Ministerio de Economía y Competitividad (RYC-2013-12587) to LG. We thank Jeremy Carver (UCSD) for assistance with proteomics data upload to MassIVE repository.

8. CONFLICT OF INTEREST DISCLOSURE

The authors declare no conflict of interest.

REFERENCES

1 Collin, M. & Bigley, V. Human dendritic cell subsets: an update. *Immunology* **154**, 3-20, doi:10.1111/imm.12888 (2018).

2 Naik, S. H. Demystifying the development of dendritic cell subtypes, a little. *Immunology and cell biology* **86**, 439-452, doi:10.1038/icb.2008.28 (2008).

3 Paul, F. & Amit, I. Plasticity in the transcriptional and epigenetic circuits regulating dendritic cell lineage specification and function. *Curr Opin Immunol* **30**, 1-8, doi:10.1016/j.coi.2014.04.004 (2014).

4 Wasylyk, B., Hahn, S. L. & Giovane, A. The Ets family of transcription factors. *Eur J Biochem* **211**, 7-18 (1993).

5 Carotta, S. *et al.* The transcription factor PU.1 controls dendritic cell development and Flt3 cytokine receptor expression in a dose-dependent manner. *Immunity* **32**, 628-641, doi:10.1016/j.immuni.2010.05.005 (2010).

6 Kanada, S. *et al.* Critical role of transcription factor PU.1 in the expression of CD80 and CD86 on dendritic cells. *Blood* **117**, 2211-2222, doi:10.1182/blood-2010-06-291898 (2011).

7 Kitamura, N. *et al.* Role of PU.1 in MHC class II expression through transcriptional regulation of class II transactivator pI in dendritic cells. *The Journal of allergy and clinical immunology* **129**, 814-824 e816, doi:10.1016/j.jaci.2011.10.019 (2012).

8 Aittomaki, S., Yang, J., Scott, E. W., Simon, M. C. & Silvennoinen, O. Molecular basis of Stat1 and PU.1 cooperation in cytokine-induced Fcgamma receptor I promoter activation. *Int Immunol* **16**, 265-274 (2004).

9 Brass, A. L., Zhu, A. Q. & Singh, H. Assembly requirements of PU.1-Pip (IRF-4) activator complexes: inhibiting function in vivo using fused dimers. *The EMBO journal* **18**, 977-991, doi:10.1093/emboj/18.4.977 (1999).

10 Hodawadekar, S., Park, K., Farrar, M. A. & Atchison, M. L. A developmentally controlled competitive STAT5-PU.1 DNA binding mechanism regulates activity of the Ig kappa E3' enhancer. *Journal of immunology* **188**, 2276-2284, doi:10.4049/jimmunol.1102239 (2012).

11 Nika, E. *et al.* hnRNP K in PU.1-containing complexes recruited at the CD11b promoter: a distinct role in modulating granulocytic and monocytic differentiation of AML-derived cells. *Biochem J* **463**, 115-122, doi:10.1042/BJ20140358 (2014).

12 Park, J. S., Jung, S. H., Seo, H. & Kim, H. S. SB203580 enhances interleukin-1 receptor antagonist gene expression in IFN-gamma-stimulated BV2 microglial cells through a composite nuclear factor-kappaB/PU.1 binding site. *Neurosci Lett* **416**, 169-174, doi:10.1016/j.neulet.2007.02.005 (2007).

13 Saliba, D. G. *et al.* IRF5:RelA interaction targets inflammatory genes in macrophages. *Cell Rep* **8**, 1308-1317, doi:10.1016/j.celrep.2014.07.034 (2014).

14 Zhang, P. *et al.* Negative cross-talk between hematopoietic regulators: GATA proteins repress PU.1. *Proceedings of the National Academy of Sciences of the United States of America* **96**, 8705-8710 (1999).

15 Gu, X. *et al.* Runx1 regulation of Pu.1 corepressor/coactivator exchange identifies specific molecular targets for leukemia differentiation therapy. *The Journal of biological chemistry* **289**, 14881-14895, doi:10.1074/jbc.M114.562447 (2014).

16 Sabado, R. L., Balan, S. & Bhardwaj, N. Dendritic cell-based immunotherapy. *Cell Res* **27**, 74-95, doi:10.1038/cr.2016.157 (2017).

17 Lundberg, K. *et al.* Transcriptional profiling of human dendritic cell populations and models--unique profiles of in vitro dendritic cells and implications on functionality and applicability. *PloS one* **8**, e52875, doi:10.1371/journal.pone.0052875 (2013).

18 Schreibelt, G. *et al.* Effective Clinical Responses in Metastatic Melanoma Patients after Vaccination with Primary Myeloid Dendritic Cells. *Clin Cancer Res* **22**, 2155-2166, doi:10.1158/1078-0432.CCR-15-2205 (2016).

19 Tel, J. *et al.* Natural human plasmacytoid dendritic cells induce antigen-specific T-cell responses in melanoma patients. *Cancer Res* **73**, 1063-1075, doi:10.1158/0008-5472.CAN-12-2583 (2013).

20 Bedke, N. *et al.* A method for the generation of large numbers of dendritic cells from CD34+ hematopoietic stem cells from cord blood. *Journal of immunological methods* **477**, 112703, doi:10.1016/j.jim.2019.112703 (2020).

21 Balan, S. *et al.* Large-Scale Human Dendritic Cell Differentiation Revealing Notch-Dependent Lineage Bifurcation and Heterogeneity. *Cell Rep* **24**, 1902-1915 e1906, doi:10.1016/j.celrep.2018.07.033 (2018).

22 Kirkling, M. E. *et al.* Notch Signaling Facilitates In Vitro Generation of Cross-Presenting Classical Dendritic Cells. *Cell Rep* **23**, 3658-3672 e3656, doi:10.1016/j.celrep.2018.05.068 (2018).

23 Helft, J. *et al.* GM-CSF Mouse Bone Marrow Cultures Comprise a Heterogeneous Population of CD11c(+)MHCII(+) Macrophages and Dendritic Cells. *Immunity* **42**, 1197-1211, doi:10.1016/j.immuni.2015.05.018 (2015).

24 Gobel, F. *et al.* Reciprocal role of GATA-1 and vitamin D receptor in human myeloid dendritic cell differentiation. *Blood* **114**, 3813-3821, doi:10.1182/blood-2009-03-210484 (2009).

25 Scheenstra, M. R. *et al.* Characterization of hematopoietic GATA transcription factor expression in mouse and human dendritic cells. *Blood Cells Mol Dis* **55**, 293-303, doi:10.1016/j.bcmd.2015.07.006 (2015).

26 Follows, G. A. *et al.* Epigenetic consequences of AML1-ETO action at the human c-FMS locus. *The EMBO journal* **22**, 2798-2809, doi:10.1093/emboj/cdg250 (2003).

27 Soler, E. *et al.* The genome-wide dynamics of the binding of Ldb1 complexes during erythroid differentiation. *Genes Dev* **24**, 277-289, doi:10.1101/gad.551810 (2010).

28 Langmead, B., Trapnell, C., Pop, M. & Salzberg, S. L. Ultrafast and memory-efficient alignment of short DNA sequences to the human genome. *Genome biology* **10**, R25, doi:10.1186/gb-2009-10-3-r25 (2009).

29 Li, H. *et al.* The Sequence Alignment/Map format and SAMtools. *Bioinformatics* **25**, 2078-2079, doi:10.1093/bioinformatics/btp352 (2009).

30 Zhang, Y. *et al.* Model-based analysis of ChIP-Seq (MACS). *Genome biology* **9**, R137, doi:10.1186/gb-2008-9-9-r137 (2008).

31 Bailey, T. L. *et al.* MEME SUITE: tools for motif discovery and searching. *Nucleic acids research* **37**, W202-208, doi:10.1093/nar/gkp335 (2009).

32 Ji, H., Jiang, H., Ma, W. & Wong, W. H. Using CisGenome to analyze ChIP-chip and ChIP-seq data. *Curr Protoc Bioinformatics* **Chapter 2**, Unit2 13, doi:10.1002/0471250953.bi0213s33 (2011).

33 Wang, S. *et al.* Target analysis by integration of transcriptome and ChIP-seq data with BETA. *Nature protocols* **8**, 2502-2515, doi:10.1038/nprot.2013.150 (2013).

34 Heinz, S. *et al.* Simple combinations of lineage-determining transcription factors prime cis-regulatory elements required for macrophage and B cell identities. *Molecular cell* **38**, 576-589, doi:10.1016/j.molcel.2010.05.004 (2010).

35 Scheenstra, M. R. *et al.* GATA1-Deficient Dendritic Cells Display Impaired CCL21-Dependent Migration toward Lymph Nodes Due to Reduced Levels of Polysialic Acid. *Journal of immunology* **197**, 4312-4324, doi:10.4049/jimmunol.1600103 (2016).

36 Yu, Y., Smith, M. & Pieper, R. A spinnable and automatable StageTip for high throughput peptide desalting and proteomics. (2014).

37 Cox, J. & Mann, M. MaxQuant enables high peptide identification rates, individualized p.p.b.-range mass accuracies and proteome-wide protein quantification. *Nat Biotechnol* **26**, 1367-1372, doi:10.1038/nbt.1511 (2008).

38 Cox, J. *et al.* Andromeda: a peptide search engine integrated into the MaxQuant environment. *J Proteome Res* **10**, 1794-1805, doi:10.1021/pr101065j (2011).

39 Luber, C. A. *et al.* Quantitative proteomics reveals subset-specific viral recognition in dendritic cells. *Immunity* **32**, 279-289, doi:10.1016/j.immuni.2010.01.013 (2010).

40 Zerbino, D. R. *et al.* Ensembl 2018. *Nucleic acids research* **46**, D754-D761, doi:10.1093/nar/gkx1098 (2018).

41 Han, H. *et al.* TRRUST v2: an expanded reference database of human and mouse transcriptional regulatory interactions. *Nucleic acids research* **46**, D380-D386, doi:10.1093/nar/gkx1013 (2018).

42 Szklarczyk, D. *et al.* The STRING database in 2017: quality-controlled protein-protein association networks, made broadly accessible. *Nucleic acids research* **45**, D362-D368, doi:10.1093/nar/gkw937 (2017).

43 Mi, H. *et al.* PANTHER version 11: expanded annotation data from Gene Ontology and Reactome pathways, and data analysis tool enhancements. *Nucleic acids research* **45**, D183-D189, doi:10.1093/nar/gkw1138 (2017).

44 Satpathy, A. T., Murphy, K. M. & Kc, W. Transcription factor networks in dendritic cell development. *Semin Immunol* **23**, 388-397, doi:10.1016/j.smim.2011.08.009 (2011).

45 Gutierrez, L. *et al.* Gata1 regulates dendritic-cell development and survival. *Blood* **110**, 1933-1941, doi:10.1182/blood-2006-09-048322 (2007).

46 Garber, M. *et al.* A high-throughput chromatin immunoprecipitation approach reveals principles of dynamic gene regulation in mammals. *Molecular cell* **47**, 810-822, doi:10.1016/j.molcel.2012.07.030 (2012).

47 Hallier, M., Tavitian, A. & Moreau-Gachelin, F. The transcription factor Spi-1/PU.1 binds RNA and interferes with the RNA-binding protein p54nrb. *The Journal of biological chemistry* **271**, 11177-11181 (1996).

48 Zhu, X. J., Yang, Z. F., Chen, Y., Wang, J. & Rosmarin, A. G. PU.1 is essential for CD11c expression in CD8(+)/CD8(-) lymphoid and monocyte-derived dendritic cells during GM-CSF or FLT3L-induced differentiation. *PloS one* **7**, e52141, doi:10.1371/journal.pone.0052141 (2012).

49 Amiel, E. *et al.* Inhibition of mechanistic target of rapamycin promotes dendritic cell activation and enhances therapeutic autologous vaccination in mice. *Journal of immunology* **189**, 2151-2158, doi:10.4049/jimmunol.1103741 (2012).

50 Chauvistre, H. *et al.* Dendritic cell development requires histone deacetylase activity. *European journal of immunology* **44**, 2478-2488, doi:10.1002/eji.201344150 (2014).

FIGURE LEGENDS

Figure 1. Scheme of the experimental design and culture of mouse and human inflammatory DCs

a) Experimental design and culture set up.

b) Flow cytometry analysis of cultured mouse and human inflammatory DC.

Figure 2. PU.1 Chromatin Immunoprecipitation in mouse BMDCs. Distribution of identified peaks, assigned genes and overlay with RNA-Seq data

a) Euler diagram of identified peaks of PU.1 binding after PU.1 ChIP-Seq analysis. Green circle: identified peaks in steady state (ST) BMDCs. Red circle: identified peaks in LPS-stimulated BMDCs. Numbers on each section indicate the peaks identified only in ST, only in LPS, or overlapping in both conditions. MEME analysis of target enriched DNA binding sequence in steady state (ST) and LPS-stimulated BMDCs in respective PU.1 ChIP-Seq samples is also depicted.

b) Pie charts depicting the chromosomal location of identified peaks.

c) Distribution of identified peaks on known promoters and bidirectional promoters.

d) Euler diagram representing the overlay of assigned genes putatively regulated by PU.1 as extrapolated from ChIP-Seq analysis and RNA-Seq data from BMDCs. Blue circle: expressed genes as identified in RNA-Seq analysis. Green circle: assigned genes bound by PU.1 in ST condition.

Red circle: assigned genes bound by PU.1 in LPS condition. Numbers on each section indicate the number of genes.

e) Distribution of assigned genes putatively regulated by PU.1 in steady state (ST) and LPS-stimulated BMDCs on differentially expressed (DE) genes, up- or downregulated. The pie chart indicates the number of up- (red) or downregulated (green) genes. The inner ring displays on each pie chart division the number of genes regulated by PU.1 in steady state (ST) condition (dark green), in LPS-stimulated BMDCs (dark red), in both conditions (mustard) or not regulated by PU.1 (grey). Venn diagram displaying the distribution of assigned genes from ChIP-Seq datasets, taking into account DC RNA-Seq data and up- or downregulation of given genes upon LPS stimulation, is also depicted.

Figure 3. PU.1 Chromatin Immunoprecipitation in human moDCs. Distribution of identified peaks, assigned genes and overlay with RNA-Seq data

a) Euler diagram of identified peaks of PU.1 binding after PU.1 ChIP-Seq analysis. Green circle: identified peaks in steady state (ST) moDCs. Red circle: identified peaks in LPS-stimulated moDCs. Numbers on each section indicate the peaks identified only in ST, only in LPS, or overlapping in both conditions. MEME analysis of target enriched DNA binding sequence in steady state (ST) and LPS-stimulated moDCs in respective PU.1 ChIP-Seq samples is also depicted.

b) Pie charts depicting the chromosomal location of identified peaks.

c) Distribution of identified peaks on known promoters and bidirectional promoters.

d) Euler diagram representing the overlay of assigned genes putatively regulated by PU.1 as extrapolated from ChIP-Seq analysis and RNA-Seq data from moDCs. Blue circle: expressed genes as identified in RNA-Seq analysis. Green circle: assigned genes bound by PU.1 in ST condition. Red circle: assigned genes bound by PU.1 in LPS condition. Numbers on each section indicate the number of genes.

e) Distribution of assigned genes putatively regulated by PU.1 in steady state (ST) and LPS-stimulated moDCs on differentially expressed (DE) genes, up- or downregulated. The pie chart indicates the number of up- (red) or downregulated (green) genes. The inner ring displays on each pie chart division the number of genes regulated by PU.1 in steady state (ST) condition (dark green), in LPS-stimulated moDCs (dark red), in both conditions (mustard) or not regulated by PU.1 (grey). Venn diagram displaying the distribution of assigned genes from ChIP-Seq datasets, taking into account DC RNA-Seq data and up- or downregulation of given genes upon LPS stimulation, is also depicted.

Figure 4. Interspecies comparison and overlay of PU.1 target genes (ChIP-Seq) and DC expressed genes (RNA-Seq) after mouse to human ortholog translation

a) Table indicating the number of genes after ortholog translation, mouse to human and human to mouse. For further analysis, we always overlaid human datasets with mouse-to-human translated ortholog datasets. Below, Venn diagram displaying the overlay of ChIP-Seq assigned genes in steady state (ST) and LPS stimulation conditions interspecies, after mouse-to-human ortholog translation.

b) Euler diagram representing the overlay of expressed genes (RNA-Seq) after mouse to human ortholog translation. Below, Venn diagram displaying the overlap between mouse and human datasets of differentially expressed genes (DE), up- or downregulated, after mouse to human ortholog translation.

c) Euler diagram of assigned genes commonly and putatively regulated interspecies by PU.1. Green circle: assigned genes commonly regulated by PU.1 in steady state (ST) condition. Red circle: assigned genes commonly regulated by PU.1 upon LPS stimulation. Numbers on each section indicate the peaks identified only in ST, only in LPS, or overlapping in both conditions.

d) Euler diagram representing the overlay of assigned genes commonly and putatively regulated by PU.1 as extrapolated from ChIP-Seq analysis and commonly expressed genes interspecies. Blue circle: commonly expressed genes. Green circle: assigned genes commonly regulated by PU.1 in steady state (ST) condition. Red circle: assigned genes commonly

regulated by PU.1 upon LPS stimulation. Numbers on each section indicate the number of genes.

e) Distribution of assigned genes commonly and putatively regulated by PU.1 in steady state (ST) and LPS-stimulated DCs on commonly differentially expressed (DE) genes, up- or downregulated. Pie chart indicates the number of commonly up- (red) or downregulated (green) genes. The inner ring displays on each pie chart division the number of genes commonly regulated by PU.1 in steady state (ST) condition (dark green), upon LPS stimulation (dark red), in both conditions (mustard) or not regulated by PU.1 (grey). On the right, Venn diagram displaying the overlay of commonly expressed genes, commonly up- or downregulated genes, and assigned genes commonly and putatively regulated by PU.1 either in steady state (ST) condition or upon LPS stimulation. Genes corresponding to numbers within squares are shown in Supplementary Table 2.

Figure 5. PU.1 co-immunoprecipitation in mouse BMDCs and human moDCs

a) Principal Component Analysis of PU.1 co-IP identified protein samples and IgG controls performed as described. Mouse samples (above) and human samples (below) are depicted.

b) Western blot of PU.1 and STAT5B in INPUT, PU.1 IP and supernatant fractions, in samples from mouse BMDC and human moDC cultures in ST and LPS-stimulated conditions. Representative IP experiments are shown.

c) Euler diagrams of the identified PU.1 co-IPed proteins in mouse (above) and human (below) samples. The numbers indicate the identified proteins, and their distribution amongst ST or LPS condition. Venn diagrams on the left represent the whole cell interactome, while the Venn diagrams on the right represent the nuclear PU.1 interactome.

d) Venn diagrams representing the overlay interspecies of the PU.1 interactome, after mouse translation into human orthologs (total -whole cell-and nuclear proteins). Proteins corresponding to numbers within squares (nuclear proteins) are shown in Supplementary Table 3.

Figure 6. PU.1 co-immunoprecipitation in mouse BMDCs and human moDCs

a) Scheme of Core, ST and LPS PU.1 transcription complex in mouse BMDC, after shortlisting nuclear proteins (STRING) and transcription regulators (PANTHER).

b) Scheme of Core, ST and LPS PU.1 transcription complex in human moDC, after shortlisting nuclear proteins (STRING) and transcription regulators (PANTHER).

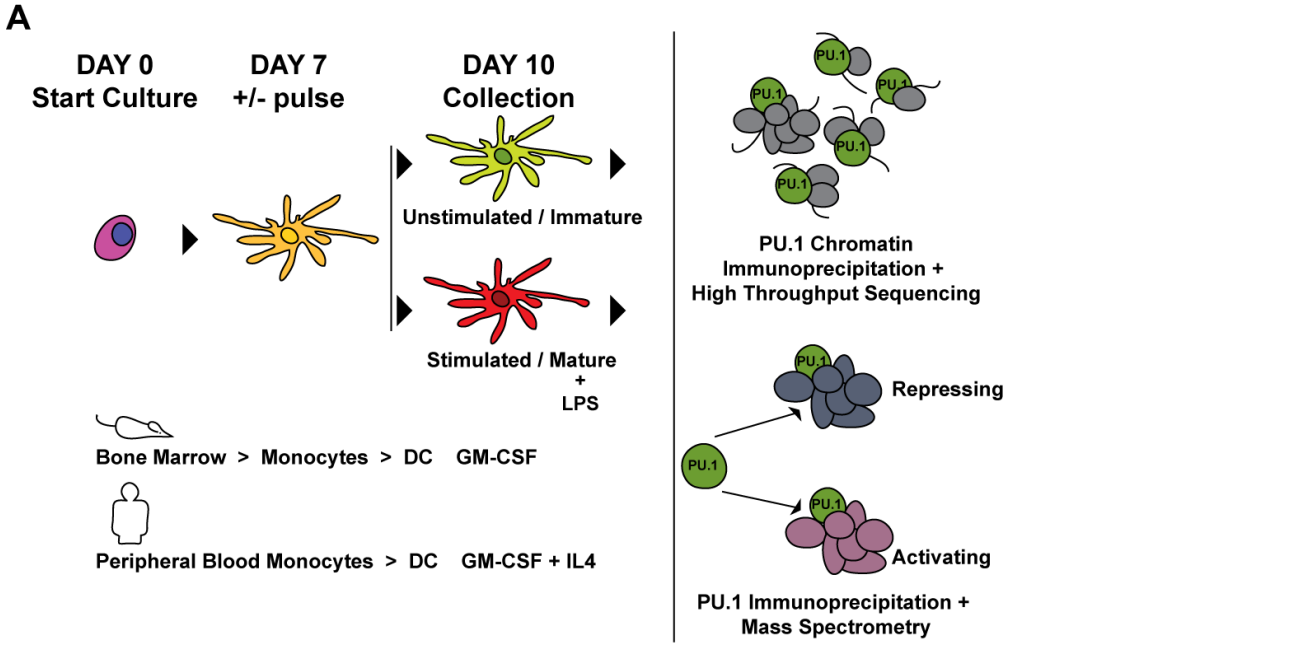
A
DAY 0
Start Culture
DAY 7
+/- pulse
DAY 10
Collection
Unstimulated / Immature
Stimulated / Mature
+
LPS
Bone Marrow > Monocytes > DC GM-CSF
Peripheral Blood Monocytes > DC GM-CSF + IL4
PU.1
PU.1 Chromatin
Immunoprecipitation +
High Throughput Sequencing
Repressing
Activating
PU.1 Immunoprecipitation +
Mass Spectrometry

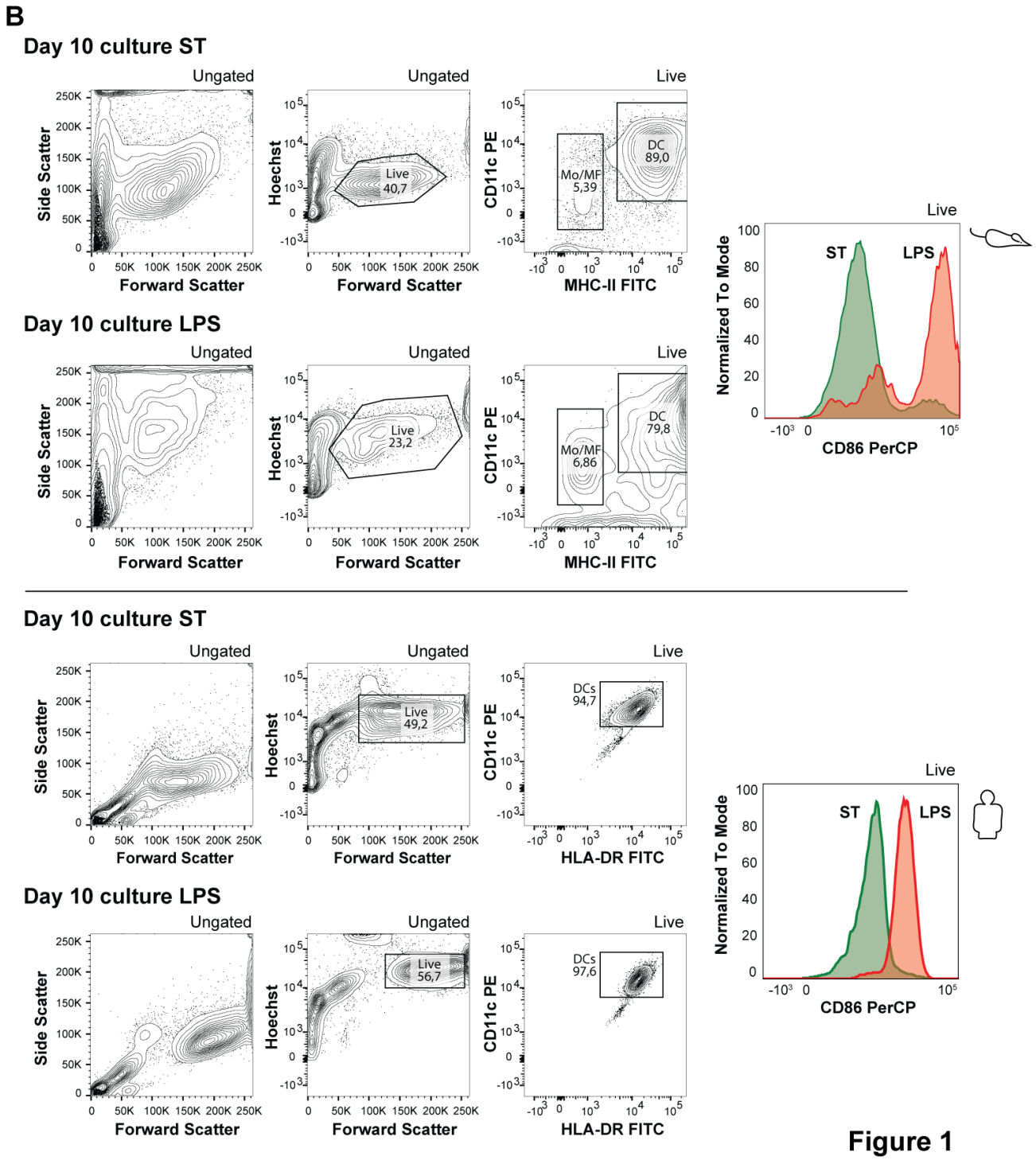
B
Day 10 culture ST
Ungated
Ungated
Live
Side Scatter
Forward Scatter
Hoechst
Live
40,7
CD11c PE
Mo/MF
5,39
DC
89,0
MHC-II FITC
Day 10 culture LPS
Live
23,2
Mo/MF
6,86
DC
79,8
Normalized To Mode
ST
LPS
CD86 PerCP
Day 10 culture ST
Live
49,2
DCs
94,7
HLA-DR FITC
Day 10 culture LPS
Live
56,7
DCs
97,6

Figure 1

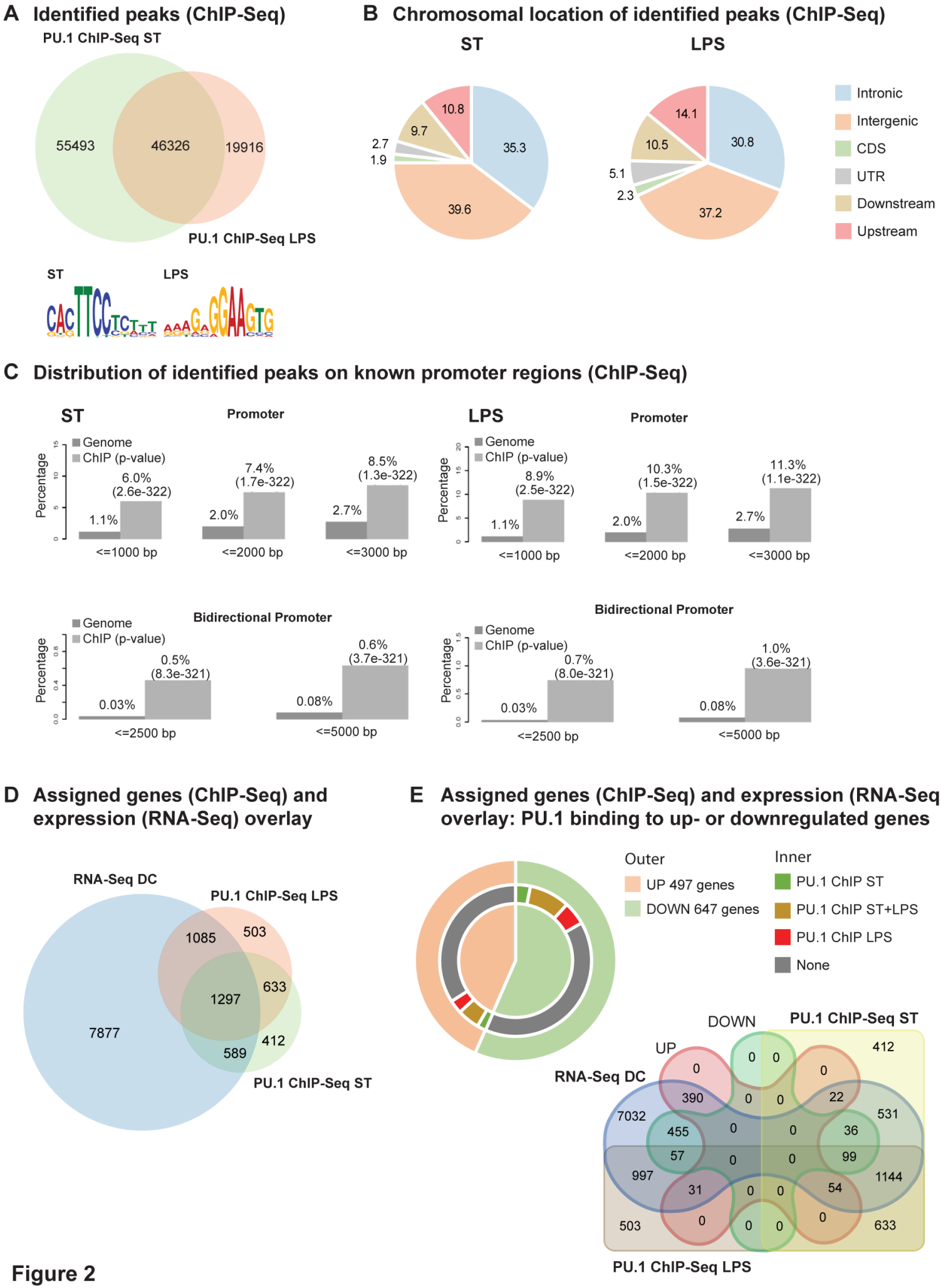
A Identified peaks (ChIP-Seq)
PU.1 ChIP-Seq ST
55493
46326
19916
PU.1 ChIP-Seq LPS
ST
LPS
B Chromosomal location of identified peaks (ChIP-Seq)
ST
LPS
10.8
9.7
2.7
1.9
35.3
39.6
14.1
10.5
5.1
2.3
30.8
37.2
Intronic
Intergenic
CDS
UTR
Downstream
Upstream
C Distribution of identified peaks on known promoter regions (ChIP-Seq)
ST
Promoter
Genome
ChIP (p-value)
Percentage
1.1%
6.0%
(2.6e-322)
2.0%
7.4%
(1.7e-322)
2.7%
8.5%
(1.3e-322)
<=1000 bp
<=2000 bp
<=3000 bp
LPS
Promoter
1.1%
8.9%
(2.5e-322)
2.0%
10.3%
(1.5e-322)
2.7%
11.3%
(1.1e-322)
Bidirectional Promoter
0.03%
0.5%
(8.3e-321)
0.08%
0.6%
(3.7e-321)
<=2500 bp
<=5000 bp
0.03%
0.7%
(8.0e-321)
0.08%
1.0%
(3.6e-321)
D Assigned genes (ChIP-Seq) and expression (RNA-Seq) overlay
RNA-Seq DC
PU.1 ChIP-Seq LPS
1085
503
1297
633
7877
412
589
PU.1 ChIP-Seq ST
E Assigned genes (ChIP-Seq) and expression (RNA-Seq) overlay: PU.1 binding to up- or downregulated genes
Outer
UP 497 genes
DOWN 647 genes
Inner
PU.1 ChIP ST
PU.1 ChIP ST+LPS
PU.1 ChIP LPS
None
DOWN
PU.1 ChIP-Seq ST
UP
RNA-Seq DC
0
0
0
0
412
390
0
0
22
7032
531
455
0
0
36
57
0
0
99
997
1144
31
0
0
54
503
0
0
0
0
633
PU.1 ChIP-Seq LPS

Figure 2

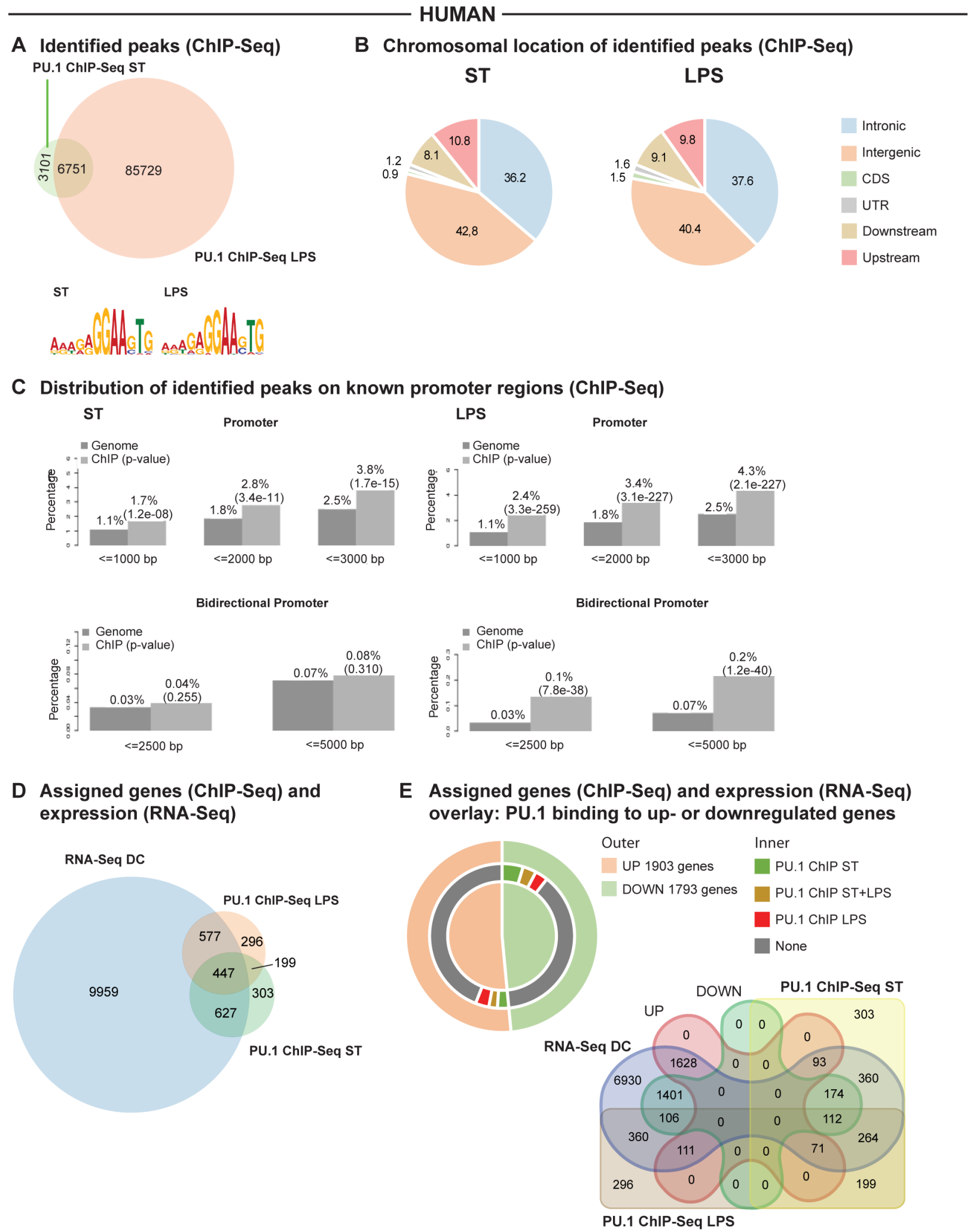
A Identified peaks (ChIP-Seq)
PU.1 ChIP-Seq ST
3101
6751
85729
PU.1 ChIP-Seq LPS
ST
LPS
B Chromosomal location of identified peaks (ChIP-Seq)
ST
LPS
10.8
8.1
1.2
0.9
36.2
42,8
9.8
9.1
1.6
1.5
37.6
40.4
Intronic
Intergenic
CDS
UTR
Downstream
Upstream
C Distribution of identified peaks on known promoter regions (ChIP-Seq)
ST
Promoter
Genome
ChIP (p-value)
Percentage
1.1%
1.7%
(1.2e-08)
1.8%
2.8%
(3.4e-11)
2.5%
3.8%
(1.7e-15)
<=1000 bp
<=2000 bp
<=3000 bp
LPS
Promoter
1.1%
2.4%
(3.3e-259)
1.8%
3.4%
(3.1e-227)
2.5%
4.3%
(2.1e-227)
Bidirectional Promoter
0.03%
0.04%
(0.255)
0.07%
0.08%
(0.310)
<=2500 bp
<=5000 bp
0.03%
0.1%
(7.8e-38)
0.07%
0.2%
(1.2e-40)
D Assigned genes (ChIP-Seq) and expression (RNA-Seq)
RNA-Seq DC
PU.1 ChIP-Seq LPS
PU.1 ChIP-Seq ST
9959
577
296
199
447
303
627
E Assigned genes (ChIP-Seq) and expression (RNA-Seq) overlay: PU.1 binding to up- or downregulated genes
Outer
UP 1903 genes
DOWN 1793 genes
Inner
PU.1 ChIP ST
PU.1 ChIP ST+LPS
PU.1 ChIP LPS
None
UP
DOWN
PU.1 ChIP-Seq ST
RNA-Seq DC
PU.1 ChIP-Seq LPS
0
1628
6930
1401
106
360
111
296
303
93
360
174
112
264
71
199

Figure 3

A Overlay Interspecies ChIP-Seq (Mm to Hs Orthologs)

	Regulated genes	Ortholog genes		Unmatched genes
Hs ST	1576	Mm	1373	203 (12,88%)
Hs LPS	1519	Mm	1320	199 (13,10%)
Mm ST	2931	Hs	2546	385 (13,16%)
Mm LPS	3518	Hs	3049	469 (13,33%)

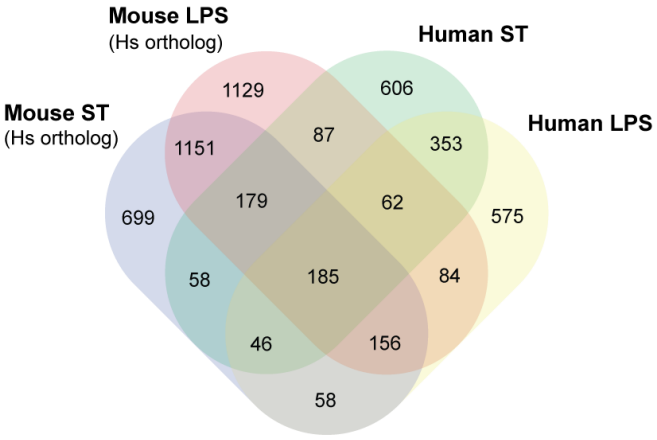

B Overlay Interspecies RNA-Seq (Mm to Hs Orthologs)

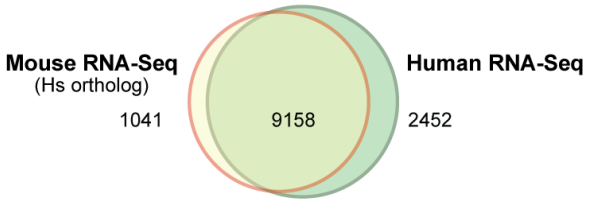

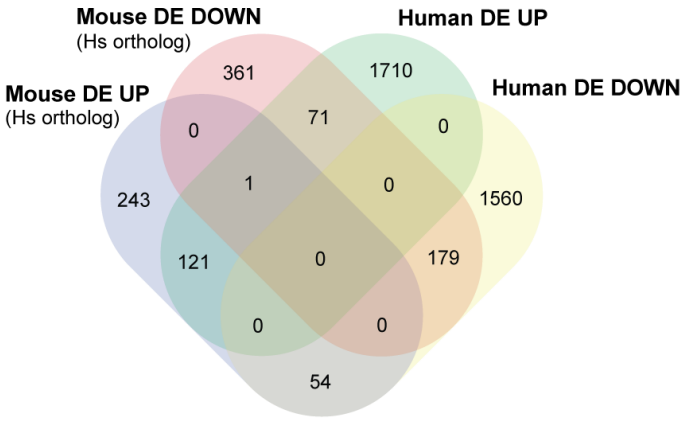

C ChIP-Seq assigned common genes (Mm to Hs Orthologs)

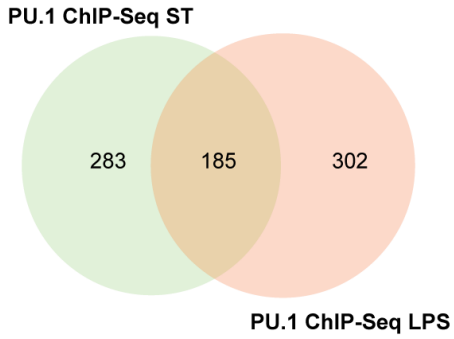

D Assigned genes (ChIP-Seq) and expression (RNA-Seq): common genes (Mm to Hs Orthologs)

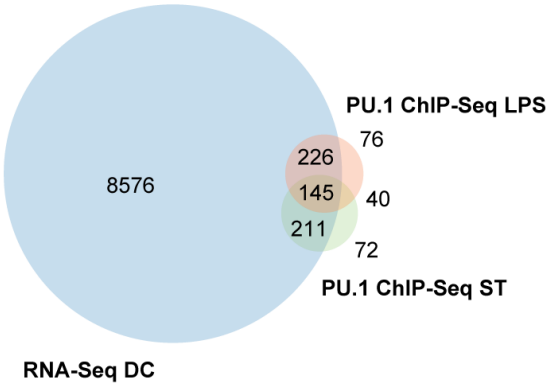

E Assigned genes (ChIP-Seq) and expression (RNA-Seq) overlay: PU.1 binding to up- or downregulated genes: common genes (Mm to Hs Orthologs)

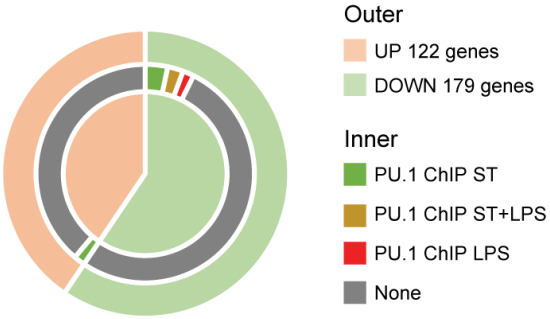

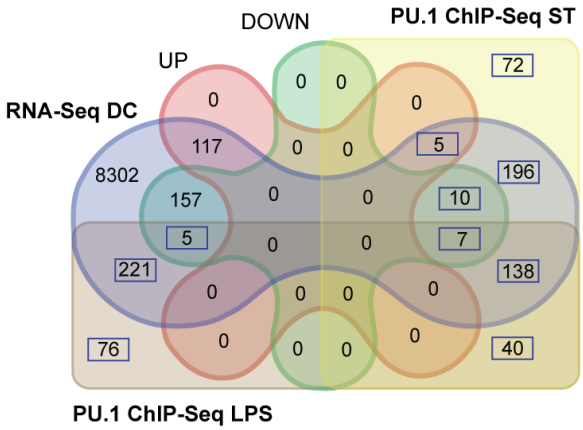

Figure 4

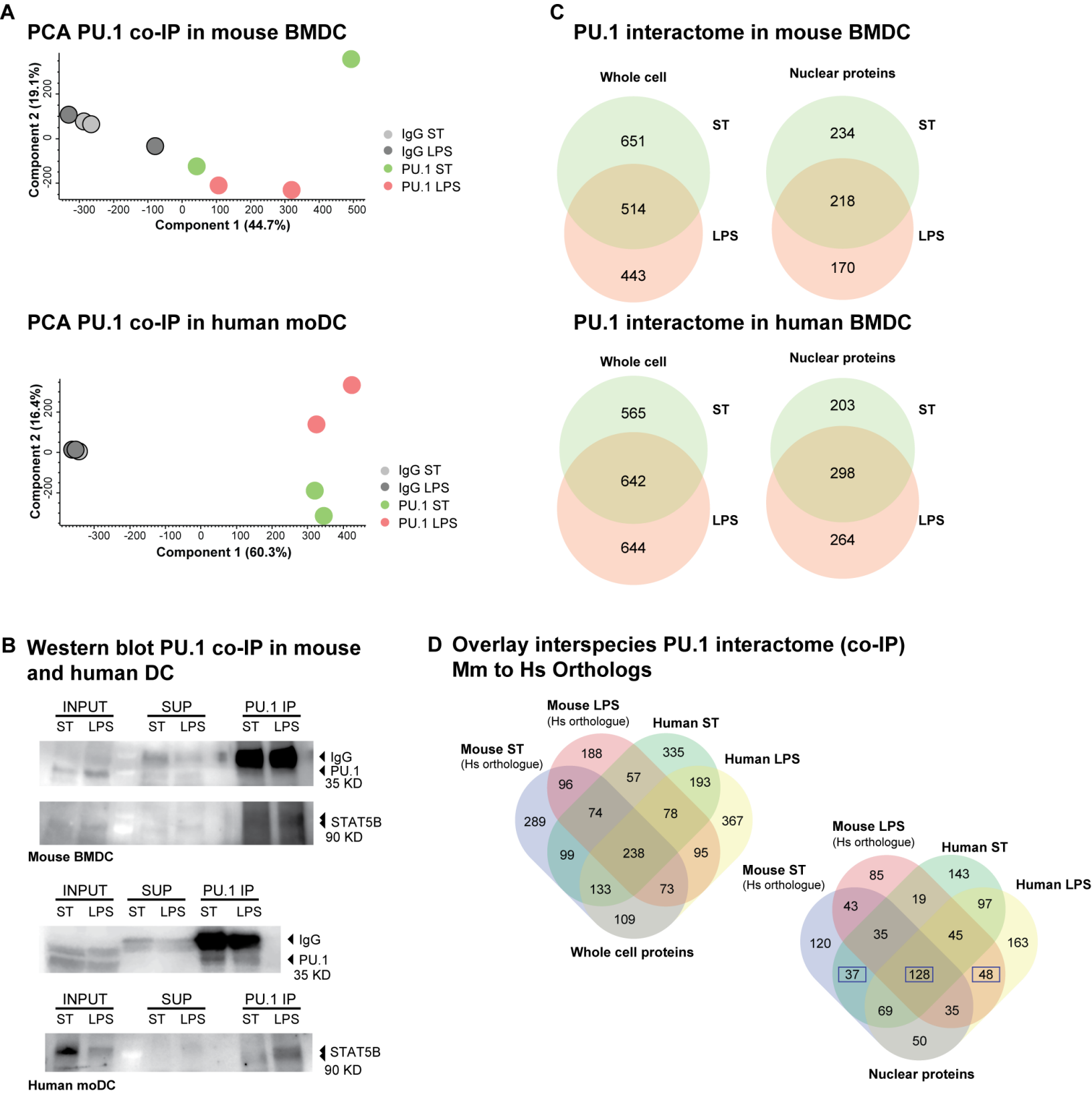
A
PCA PU.1 co-IP in mouse BMDC
Component 2 (19.1%)
Component 1 (44.7%)
IgG ST
IgG LPS
PU.1 ST
PU.1 LPS
PCA PU.1 co-IP in human moDC
Component 2 (16.4%)
Component 1 (60.3%)
IgG ST
IgG LPS
PU.1 ST
PU.1 LPS
C
PU.1 interactome in mouse BMDC
Whole cell
Nuclear proteins
ST
LPS
651
514
443
234
218
170
PU.1 interactome in human BMDC
565
642
644
203
298
264
B Western blot PU.1 co-IP in mouse and human DC
INPUT
SUP
PU.1 IP
ST LPS ST LPS ST LPS
IgG
PU.1
35 KD
STAT5B
90 KD
Mouse BMDC
Human moDC
D Overlay interspecies PU.1 interactome (co-IP) Mm to Hs Orthologs
Mouse LPS
(Hs orthologue)
Human ST
Mouse ST
(Hs orthologue)
Human LPS
188
335
96
57
193
289
74
78
367
99
238
95
133
73
109
Whole cell proteins
Mouse LPS
(Hs orthologue)
Human ST
Mouse ST
(Hs orthologue)
Human LPS
85
143
43
19
97
120
35
45
163
37
128
48
69
35
50
Nuclear proteins

Figure 5

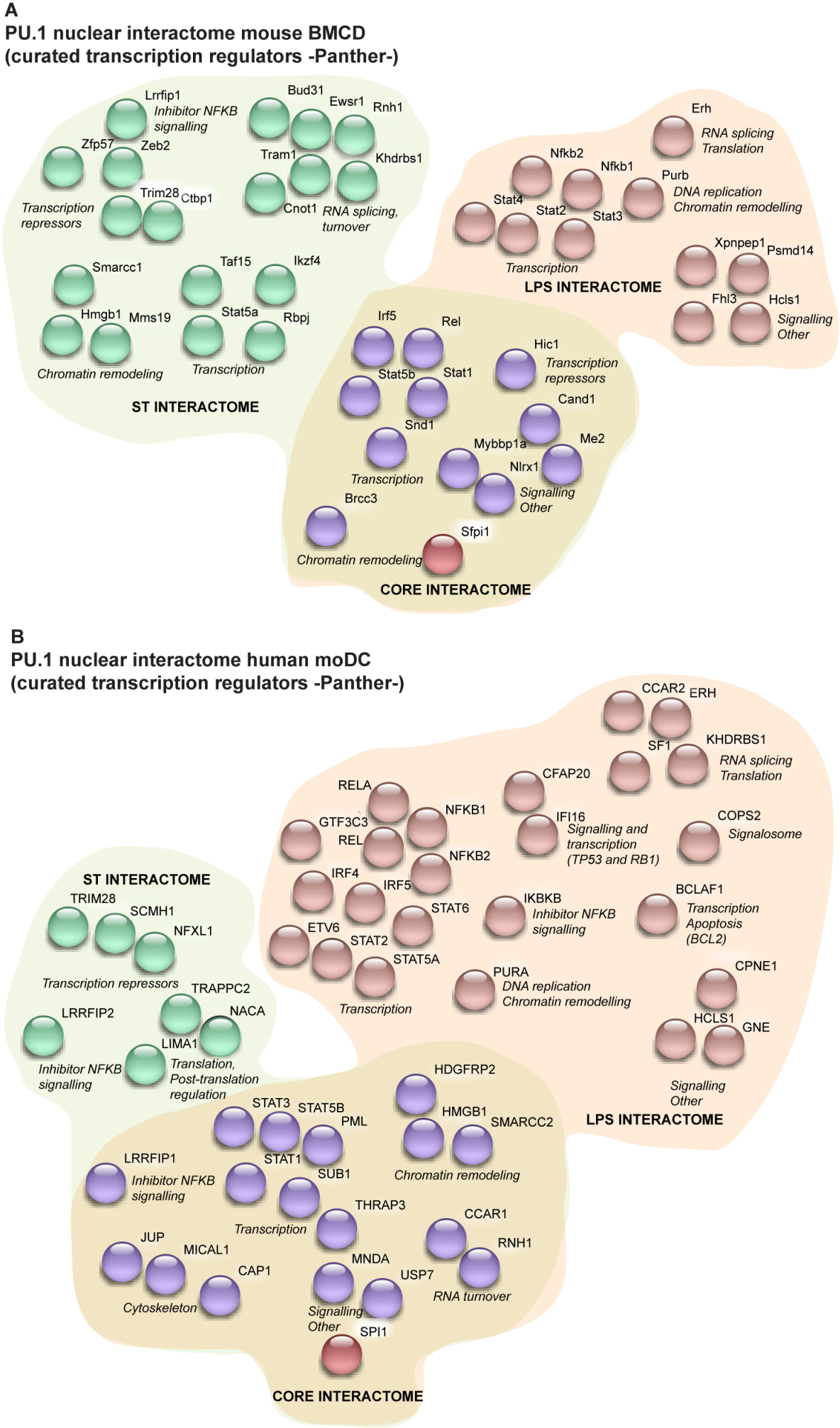
A
PU.1 nuclear interactome mouse BMCD
(curated transcription regulators -Panther-)
Lrrfip1
Inhibitor NFKB signalling
Zfp57
Zeb2
Transcription repressors
Trim28
Ctbp1
Bud31
Ewsr1
Rnh1
Tram1
Khdrbs1
Cnot1
RNA splicing, turnover
Smarcc1
Hmgb1
Mms19
Chromatin remodeling
Taf15
Ikzf4
Stat5a
Rbpj
Transcription
ST INTERACTOME
Erh
RNA splicing
Translation
Nfkb2
Nfkb1
Purb
DNA replication
Chromatin remodelling
Stat4
Stat2
Stat3
Transcription
LPS INTERACTOME
Xpnpep1
Psmd14
Fhl3
Hcls1
Signalling
Other
Irf5
Rel
Stat5b
Stat1
Hic1
Transcription repressors
Snd1
Cand1
Transcription
Mybbp1a
Me2
Nlrx1
Signalling
Other
Brcc3
Chromatin remodeling
Sfpi1
CORE INTERACTOME
B
PU.1 nuclear interactome human moDC
(curated transcription regulators -Panther-)
CCAR2
ERH
SF1
KHDRBS1
RNA splicing
Translation
CFAP20
RELA
NFKB1
GTF3C3
REL
NFKB2
IFI16
Signalling and transcription (TP53 and RB1)
COPS2
Signalosome
IRF4
IRF5
STAT6
ETV6
STAT2
STAT5A
Transcription
IKBKB
Inhibitor NFKB signalling
BCLAF1
Transcription Apoptosis (BCL2)
PURA
DNA replication
Chromatin remodelling
CPNE1
HCLS1
GNE
Signalling
Other
LPS INTERACTOME
ST INTERACTOME
TRIM28
SCMH1
NFXL1
Transcription repressors
TRAPPC2
LRRFIP2
NACA
LIMA1
Inhibitor NFKB signalling
Translation, Post-translation regulation
HDGFRP2
HMGB1
SMARCC2
Chromatin remodeling
STAT3
STAT5B
PML
STAT1
LRRFIP1
Inhibitor NFKB signalling
SUB1
Transcription
THRAP3
CCAR1
RNH1
RNA turnover
JUP
MICAL1
CAP1
Cytoskeleton
MNDA
USP7
Signalling
Other
SPI1
CORE INTERACTOME

Figure 6